Earth Syst. Sci. Data Discuss., doi:10.5194/essd-2016-22, 2016
Manuscript under review for journal Earth Syst. Sci. Data
Published: 17 June 2016

Global Ocean Particulate Organic Carbon Flux Merged with Satellite Parameters

Colleen B. Mouw[1*], Audrey Barnett[1], Galen A. McKinley[2], Lucas Gloege[2], Darren Pilcher[3]

[1]Michigan Technological University
1400 Townsend Drive
Houghton, MI 49931
USA

[2]University of Wisconsin-Madison
1225 W. Dayton Street
Madison, WI 53706
USA

[3]NOAA, Pacific Marine Environmental Laboratory
7600 Sand Point Way NE
Seattle, WA 98115

[*]Corresponding author, cbmouw@mtu.edu, +1 906-487-2795

Earth Syst. Sci. Data Discuss., doi:10.5194/essd-2016-22, 2016
Manuscript under review for journal Earth Syst. Sci. Data
Published: 17 June 2016

Abstract

Particulate organic carbon (POC) flux estimated from POC concentration observations from sediment traps and ^{234}Th are compiled across the global ocean. The compilation includes six time series locations: CARIACO, K2, OSP, BATS, OFP and HOT. Efficiency of the biological pump of carbon to the deep ocean depends largely on biologically mediated export of carbon from the surface ocean and its remineralization with depth, thus biologically related parameters able to be estimated from satellite observations were merged at the POC observation sites. Satellite parameters include: net primary production, percent microplankton, sea surface temperature, photosynthetically active radiation, diffuse attenuation coefficient at 490 nm, euphotic zone depth, as well as, climatological mixed layer depth. 85% of the observations across the globe are concentrated in the Northern Hemisphere with 44% of the data record overlapping the satellite record. Time series sites accounted for 36% of the data. 71% of the data is measured at ≥500 m with the most common deployment depths between 1000 and 1500 m. This dataset is valuable for investigations of CO_2 drawdown, carbon export, remineralization, and sequestration. The compiled data can be freely accessed at doi: 10.1594/PANGAEA.855600.

Keywords: POC flux, phytoplankton size, microplankton fraction, S_{fm}, chlorophyll concentration, net primary production, sea surface temperature, diffuse attenuation coefficient, euphotic depth, photosynthetically available radiation, mixed layer depth

Earth Syst. Sci. Data Discuss., doi:10.5194/essd-2016-22, 2016
Manuscript under review for journal Earth Syst. Sci. Data
Published: 17 June 2016

1. Introduction

Particulate organic carbon (POC) flux estimated from POC concentration observations have been made over many decades in the interest of understanding the biological pump of carbon to the deep ocean. While there have been a variety of new techniques to observe POC concentration to estimate POC flux, sediment traps have been the most extensive temporally and geographically, while 234-Thorium has improved data resolution in the upper 500 m of the water column. POC flux depends largely on the biologically mediated export of carbon from the surface ocean and its remineralization with depth, thus capturing biological variables associated with POC flux are essential to understand flux variability. Here we compile POC flux estimated from sediment traps and 234-Thorium from around the globe from public repositories and directly in the literature. We then match the POC flux with biological and physical parameters determined from satellite imagery along with mixed layer depth climatology. See Table 1 for a list of products and units.

2. Data and Methodology

2.1. Satellite products and mixed layer depth

We provide products derived from SeaWiFS (Sea-viewing Wide Field-of-view Sensor) monthly global area coverage (GAC, level 3 mapped data, 9 km, 8-day resolution, version R2010.0) imagery over the mission record (September 1997 – December 2010) acquired from NASA Ocean Biology Distributed Active Archive Center (OB.DAAC) (http://oceancolor.gsfc.nasa.gov/). These include: chlorophyll concentration ([Chl]) (Maritorena et al., 2002), diffuse attenuation coefficient at 490 nm ($K_d(490)$) (O'Reilly et al., 2000) and photosynthetically available radiation (PAR) (Frouin et al. 2002). At the time of writing, only

8% of the publically available POC observations were measured beyond 2008, when the MODerate resolution Imaging Spectroradiometer (MODIS) replaced the SeaWiFS record, thus we focus our data compilation here solely on SeaWiFS. Net primary production (NPP) estimates from the Vertically Generalized Production Model (VGPM) (Behrenfeld and Falkowski, 1997) are obtained from http://www.science.oregonstate.edu/ocean.productivity/. AVHRR Pathfinder Version 5 sea surface temperature (SST) imagery was acquired from the US National Oceanographic Data Center and GHRSST (http://pathfinder.nodc.noaa.gov) (Casey et al., 2010). Satellite data products are retrieved as the median of a 5x5 pixel box centered on each time-series location (Bailey and Werdell, 2006).

The Mouw and Yoder (2010) approach is used for satellite retrieval of phytoplankton size classes. The method estimates the percentage of microplankton (S_{fm}) from satellite imagery of remote sensing reflectance ($R_{rs}(\lambda)$). This is an absorption-based approach where the chlorophyll-specific absorption spectra for phytoplankton size class extremes, pico- (0.2–2 μm) and microplankton (>20 μm), are weighted by S_{fm} (Ciotti et al., 2002; Ciotti and Bricaud, 2006). Briefly, S_{fm} is estimated from a look-up-table containing simulated chlorophyll [Chl], absorption due to dissolved and detrital material at 443 nm ($a_{cdm}(443)$), $R_{rs}(\lambda)$, and S_{fm}. For a given pixel, satellite estimated [Chl] and $a_{cdm}(443)$ (Maritorena et al., 2002) are used to narrow the search space within the look-up-table. Of the remaining options, the closest simulated $R_{rs}(\lambda)$ to the satellite observed $R_{rs}(\lambda)$ is selected and the associated S_{fm} is assigned.

Export depth is often chosen as either the base of the euphotic zone or mixed layer depth (Lutz et al. 2007, Lam et al., 2011), thus both are complied here. The depth of the euphotic zone was determined from $K_d(490)$ (O'Reilly et al., 2000) as $4.6/K_d(490)$ (Morel and Berthon, 1989). Mixed layer depth (MLD) estimates are obtained from the level 3 global monthly climatology

Earth Syst. Sci. Data Discuss., doi:10.5194/essd-2016-22, 2016
Manuscript under review for journal Earth Syst. Sci. Data
Published: 17 June 2016

data product from the IFREMER/LOS Mixed Layer Depth Climatology group (www.ifremer.fr/cerweb/deboyer/mld). We utilize MLD climatology retrieved from density profiles using a variable density threshold equivalent to 0.2°C, which accounts for both changes in temperature and salinity (de Boyer Montégut et al., 2004; de Boyer Montégut et al., 2007; Mignot et al., 2007).

2.2 POC flux data

POC sediment trap data is acquired from public repositories and published literature (Table 2; Figure 1). Estimates from ^{234}Th measurements are also acquired to improve the resolution of observations in the upper 500 m of the water column (Dunne et al., 2005; Henson et al., 2012; Guidi et al., 2015). These represent 2% of the total data set. Collected estimates of POC flux derived from ^{234}Th maintain the original authors' analysis, where POC flux is retrieved based on ^{234}Th activity in the water column accounting for the ratio of POC to ^{234}Th concentration (Buesseler et al., 2009). A significant number of studies occurred prior to the launch of SeaWiFS in September 1997 (see Honjo et al., 2008 and references therein). While we compiled observations across all available timeframes, greater focus is placed on collecting data concurrent with the satellite record to allow corresponding imagery-based environmental parameters to be matched. Overall, the data set comprises a total of 15,862 individual measurements at 623 unique locations with 6,938 (44%) collected during the satellite record. In the interest of matching the time scale of POC flux to monthly satellite-derived products to the greatest degree possible, we focused on collecting short-term deployments with individual cup intervals of 30 days or less. The majority of the dataset (14,210 measurements or 90%) fell into this category with a median cup interval of 14 days and a standard deviation of 6 days. Data are

Earth Syst. Sci. Data Discuss., doi:10.5194/essd-2016-22, 2016
Manuscript under review for journal Earth Syst. Sci. Data
Published: 17 June 2016

skewed towards shorter deployments with 60% of qualified measurements deployed 14 days or less and 96% deployed 20 days or less.

2.3 Time-series sites

Six long-term oceanographic time series locations are included in the compilation, providing detailed temporal resolution of POC flux export and remineralization. These were: the Carbon Retention In A Colored Ocean (CARIACO) project site in the Cariaco Basin (10.5°N, 64.7°W), K2 in the northwest Pacific (47°N, 160°E), Ocean Station Papa (50°N, 145°W), the Bermuda Atlantic Time Series (BATS) study site in the Sargasso Sea (31.7°N, 64.2°W), the Ocean Flux Program (OFP, 31.8°N, 64.2°W) and the Hawaii Ocean Time series (HOT, 22.8°N, 158.0°W). Data from BATS and OFP could be combined to create a complete water column profile with BATS sediment traps deployed ≤300 m and OFP traps deployed ≥500 m. Also, with the exception of the first deployment year, HOT only reports POC flux at a single depth.

2.4 Fluxes of other constituents, uncertainty estimates and metadata

Where readily available, we collect concurrent flux estimates of other organic and inorganic components in addition to POC flux including particulate inorganic carbon, particulate nitrogen and phosphorus, calcium carbonate, biogenic silica, trace metals and phytoplankton pigments (Table 1). These data are included to explore relationships between POC export and remineralization and ballasting materials. Where reported by the original authors, we include uncertainty estimates for measured fluxes in the compilation. We also collect and include metadata as reported by the original authors. At a minimum, we require each observation be associated with latitude and longitude, deployment date and depth to be included in the dataset. Other information, such as sediment trap type and trap funnel area are included where available.

Earth Syst. Sci. Data Discuss., doi:10.5194/essd-2016-22, 2016
Manuscript under review for journal Earth Syst. Sci. Data
Published: 17 June 2016

Open Access Earth System Science Data Discussions

3. Results

The deployment, retrieval and analysis of sediment trap and ^{234}Th samples represents a significant expenditure of both effort and resources and projects are often funded on a short-term local/regional basis (Honjo et al., 2008). This is reflected in the patchy distribution of observations across the globe in multiple dimensions: space, time and vertical resolution (Figure 1). Collection efforts are more prevalent in the Northern Hemisphere, with 64% of unique station locations comprising 85% of total observations falling north of the equator (Figure 2a and 2b). Long-term oceanographic time series locations at BATS/OFP, CARIACO, K2, OSP and HOT (all in the Northern Hemisphere) collectively account for 36% of the total dataset. If time series locations are removed, 77% of remaining observations still concentrate north of the equator. The most sampled regions in the Northern Hemisphere are at mid-latitudes, with a quarter of the dataset (discounting time series locations) falling between 30 and 40°N (Figure 2b). In the Southern Hemisphere, data are concentrated at higher latitudes, with a little over half of collected measurements derived from the Southern Ocean at ≥60°S. In both hemispheres, the second most sampled latitudes are near the equator (10°N–10°S).

The dataset spans four decades from 1976 to 2012 with the majority of efforts (59%) deployed between 1990 and 2000 (Figure 2, Table 2). In addition, 44% of the measurements were collected after September 1997, when the SeaWiFS mission was launched. Prior to SeaWiFS, 79% of observations are in the Northern Hemisphere (Figure 2c). Concurrent with the satellite record, the latitudinal distribution becomes even more skewed with 93% of the observations in the Northern Hemisphere (Figure 2d).

While 44% of the data was observed during the continuous satellite era (beginning September 1997), not all observations had coincidental imagery. Here we define coincident as

Earth Syst. Sci. Data Discuss., doi:10.5194/essd-2016-22, 2016
Manuscript under review for journal Earth Syst. Sci. Data
Published: 17 June 2016

the presence of pixels in a 5x5 pixel box surrounding the observation location within the same month as trap deployment or ^{234}Th measurement. We consider only the S_{fm} and NPP imagery for this purpose as they are representative of phytoplankton surface processes and the NPP product already requires SST and [Chl] imagery as inputs. This reduces the total satellite era observations from 6,938 to 3,781; a drop in total contribution from 44% to 24%. These are spread over 245 unique locations (Figure 3). Of the coincident observations, 95% are in the Northern Hemisphere primarily between 10°N and 50°N, with the majority found between 30°N and 40°N (Figure 2e). Data sets in some regions of the ocean (e.g. the equatorial Pacific and the Arabian Sea in Figure 1) have no satellite overlap (Figure 3).

The depth resolution of the observations is important for investigators interested in fitting export flux relationships (Martin et al., 1987; Lima et al., 2014). The greatest variability in POC flux is found in the first 500 m of the water column (Lam et al., 2011, Figure 4). Considering all the POC observations together, the median POC flux rapidly diminishes from 160 mg C m^{-2} d^{-1} in the upper 100 m to 30 mg C m^{-2} d^{-1} at 500 m and 6 mg C m^{-2} d^{-1} at 1000 m. Below 1000 m, the average POC flux is 3 mg C m^{-2} d^{-1} (Figure 4).

Overall, 71% of the compiled dataset is measured at ≥500 m (Figure 5). Thus, the upper water column close to the depth of export is relatively underrepresented. To increase depth resolution, we consider ^{234}Th and sediment traps together (Dunne et al., 2005; Guidi et al., 2015). Guidi et al. (2015) also merged data from the underwater vision profiler (UVP), which we did not include in this compilation as it has not yet been released into a public archive. Shallow observations are critical for capturing the impact of phytoplankton on POC export flux as these data are most connected to surface processes. By adding ^{234}Th measurements to the dataset, 74 locations gain depths in the upper water column <500 m. ^{234}Th data contribute 25% of all POC

Earth Syst. Sci. Data Discuss., doi:10.5194/essd-2016-22, 2016
Manuscript under review for journal Earth Syst. Sci. Data
Published: 17 June 2016

flux estimates resolved at depths between 100 and 200 m (Figure 5a). Overall, the most common deployment depths are between 1000 and 1500 m (14%) followed by 200 to 300 m (10%) and then 3000 to 3500 m (9%) (Figure 5b). The dominance of the 1000 to 1500 m observation depth is weighted to the pre-satellite era (Figure 5c). During the satellite era, 200 to 300 m (6%) became the most sampled depth, largely due to persistent time series observations at BATS and OSP, followed closely by the 1000 to 1500 m and 3000 to 3500 m bins (5% each) again the result of time series observations at CARIACO and OFP (Figure 5d). Reasonable depth resolution is found in the observations coincident with satellite matchups (Figure 5d).

4. Conclusions

This dataset is the most comprehensive compilation of POC flux across the globe that we are aware of. By providing merged coincident satellite imagery products, the dataset can immediately be used to link phytoplankton surface process with POC flux. Due to rapid remineralization within the first 500 m of the water column, shallow observations from 234-Thorium are helpful to supplement the more extensive sediment trap record. The data compilation is also insightful in terms of spatial and depth resolution to aid in decision making for future POC flux observing investments.

Earth Syst. Sci. Data Discuss., doi:10.5194/essd-2016-22, 2016
Manuscript under review for journal Earth Syst. Sci. Data
Published: 17 June 2016

Data Availability

The dataset contains 15,862 individual POC flux estimates at 623 unique locations collected between 1976 and 2012. Where available, the flux of other minerals was also reported. 44% (6,938) of the observations overlapped the SeaWiFS satellite record (September 1997 to December 2010). Satellite parameters extracted as the median of a 5x5 pixel box were associated with the observation sites. Satellite parameters provided in this compilation include: chlorophyll concentration, net primary production, sea surface temperature, diffuse attenuation coefficient, euphotic depth, photosynthetically active radiation, microplankton fraction and mixed layer depth. The compiled data is available on PANGAEA (https://www.pangaea.de/): doi:10.1594/PANGAEA.860474 (Mouw et al., 2015).

Author Contribution

Mouw and McKinley conceived the project and acquired funding for the effort. Mouw and Barnett designed the data compilation. Barnett retrieved and processed all data and prepared figures. Mouw and Barnett prepared the manuscript with contributions from all co-authors.

Acknowledgements

We would like to thank the Ocean Color Processing Group at NASA GSFC for the processing and distribution of the SeaWiFS imagery and the IFREMER/LOS Mixed Layer Depth Climatology group for retrieval and distribution of MLD estimates. We would also like to thank BCO-DMO, NOAA National Centers for Environmental Information, the U.S. JGOFS Data System at WHOI, JAMSTEC, Fisheries and Oceans Canada and the time-series efforts at BATS, OFP, OSP, CARIACO and HOT for continued collection and hosting of publicly available data

Earth Syst. Sci. Data Discuss., doi:10.5194/essd-2016-22, 2016
Manuscript under review for journal Earth Syst. Sci. Data
Published: 17 June 2016

sets. We would like to thank Makio C. Honda for sending data from locations in the northwest Pacific, Walker O. Smith Jr. for sharing data from the Ross Sea, Maureen Conte for sharing the OFP archive and David Timothy and Roy Hourston for providing the OSP dataset. The National Aeronautics and Space Administration (NNX11AD59G and NNX13AC34G) provided financial support for this data compilation effort. This is contribution number 38 of the Great Lakes Research Center at Michigan Technological University.

Earth Syst. Sci. Data Discuss., doi:10.5194/essd-2016-22, 2016
Manuscript under review for journal Earth Syst. Sci. Data
Published: 17 June 2016

References

Bailey, S., and P. Werdell (2006), A multi-sensor approach for the on-orbit validation of ocean color satellite data products. *Remote Sensing Environ.*, *102*(1-2), 12–23. doi:10.1016/j.rse.2006.01.015.

Behrenfeld, M., and P. Falkowski (1997), Photosynthetic rates derived from satellite-based chlorophyll concentration. *Limnol. Oceanogr.*, *42*(1), 1–20.

Buesseler, K. O., and P. W. Boyd (2009), Shedding light on processes that control particle export and flux attenuation in the twilight zone of the open ocean. *Limnol. Oceanogr.*, 54(4), 1210-1232.

Casey, K. S., Brandon, T. B., Cornillon, P., & Evans, R. (2010). The Past, Present, and Future of the AVHRR Pathfinder SST Program. In *Oceanography from Space* (pp. 273–287). Dordrecht: Springer Netherlands. http://doi.org/10.1007/978-90-481-8681-5_16.

Church, M. J., and D. M. Karl (2013), Primary production and sediment trap flux measurements and calculations by the Hawaii Ocean Time-series (HOT) program at Station ALOHA in the North Pacific 100 miles north of Oahu, Hawaii for Cruises HOT1-227 during 1988-2010. *NOAA National Centers for Environmental Information*. Accession: 0089168. iPub: 07 March 2013. Accessed: 14 May 2012. http://data.nodc.noaa.gov/accession/0089168.

Ciotti, A., and A. Bricaud (2006), Retrievals of a size parameter for phytoplankton and spectral light absorption by colored detrital matter from water-leaving radiances at SeaWiFS channels in a continental shelf region off Brazil. *Limnol. Oceanogr.: Methods*, *4*, 237–253.

Ciotti, A., M. Lewis, and J. Cullen (2002), Assessment of the relationship between dominant cell size in natural phytoplankton communities and the spectral shape of the absorption coefficient. *Limnol. Oceanogr.*, *47*(2), 404–417.

Collier, R., and J. Dymond (1994a), Sed_trap_annual. *Biological and Chemical Oceanography Data System*. BCO DMO, WHOI. iPub: 7 June 1994. Accessed: 17 September 2013. http://www.bco-dmo.org/dataset/2608.

Collier, R., and J. Dymond (1994b), Sed_trap_Eq_North. *Biological and Chemical Oceanography Data System*. BCO DMO, WHOI. iPub: 9 June 1994. Accessed: 17 September 2013. http://www.bco-dmo.org/dataset/2609.

Collier, R., J. Dymond, S. Honjo, S. Manganini, R. Francois and R. Dunbar (2000), The vertical flux of biogenic and lithogenic material in the Ross Sea: moored sediment trap observations 1996-1998. *Deep Sea Res. II*, 47, 3491-3520, doi:10.1016/S0967-0645(00)00076-X.

Collins, L. E., W. Berelson, D. E. Hammond, A. Knapp, R. Schwartz and D. Capone (2011), Particle fluxes in San Pedro Basin, California: A four-year record of sedimentation and physical forcing. *Deep Sea Res. I*, 58, 898-914. doi: 10.1016/j.dsr.2011.06.008.

Conte, M. (2015), POC flux from the Ocean Flux Program. Personal Communication: 01 September 2015. See also: *Biological and Chemical Oceanography Data System*. BCO DMO, WHOI. http://www.bco-dmo.org/program/2036.

de Boyer Montégut, C., G. Madec, A. S. Fischer, A. Lazar, and D. Iudicone (2004), Mixed layer depth over the global ocean: an examination of profile data and a profile-based climatology. *J. Geophys. Res.*, 109(C12003). doi:10.1029/2004JC002378.

Earth Syst. Sci. Data Discuss., doi:10.5194/essd-2016-22, 2016
Manuscript under review for journal Earth Syst. Sci. Data
Published: 17 June 2016

de Boyer Montégut, C., J. Mignot, A. Lazar, and S. Cravatte (2007), Control of salinity on the mixed layer depth in the world ocean: 1. General description. *J. Geophys. Res.*, 112(C06011). doi:10.1029/2006JC003953.

Dunne, J., R. Armstrong, A. Gnanadesikan, and J. Sarmiento (2005), Empirical and mechanistic models for the particle export ratio. *Global Biogeochem. Cycles*, *19*(GB4026), doi:10.1029/2004GB002390.

Frouin, R., Franz, B. A., & Werdell, P. J. (2002). The SeaWiFS PAR product. ,In: S.B. Hooker and E.R. Firestone, Algorithm Updates for the Fourth SeaWiFS Data Reprocessing, NASA Tech. Memo. 2003–206892, Volume 22, NASA Goddard Space Flight Center, Greenbelt, Maryland, 46-50.

Guidi, L., Legendre, L., Reygondeau, G., Uitz, J., Stemmann, L., & Henson, S. A. (2015). A new look at ocean carbon remineralization for estimating deepwater sequestration. *Global Biogeochem. Cycles*, 1–16. http://doi.org/10.1002/2014GB005063.

Henson, S. A., R. Sanders, E. Madsen, P. J. Morris, F. Le Moigne and G. D. Quartly (2011), A reduced estimate of the strength of the ocean's biological carbon pump. *Geophys. Res. Let.*, 38, L04606, doi:10.1029/2011GL046735.

Henson, S. A., R. Sanders, and E. Madsen (2012), Global patterns in efficiency of particulate organic carbon export and transfer to the deep ocean. *Global Biogeochem. Cycles*, *26*(1), n–a–n–a. doi:10.1029/2011GB004099.

Honda, M. C. (2012), JAMSTEC Sediment trap data at time-series stations: K2 and S1 for Ocean SITES. *JAMSTEC Environmental Biogeochemical Cycle Research Program*. iPub: November 2012. Accessed: 10 April 2014. http://ebcrpa.jamstec.go.jp/rigc/e/ebcrp/mbcrt/st_k2s1_oceansites/.

Honda, M. C., K. Imai, Y. Norjiri, F. Hoshi, T. Sugawara and M. Kusakabe (2002), The biological pump in the northwestern North Pacific based on fluxes and major components of particulate matter obtained by sediment-trap experiments (1997-2000). *Deep Sea Res. II*, 49, 5595-5625, doi:10.1016/S0967-0645(02)00201-1.

Honjo, S. (1999), Sediment Properties and other data from a fixed platform from 19941102 to 19951205. *NOAA National Centers for Environmental Information*. Accession: 9800155. iPub: 15 June 1999. Accessed: 03 October 2013. http://www.nodc.noaa.gov/cgi-bin/OAS/prd/accession/9800155.

Honjo, S., and J. Dymond (1994), Sed_trap_Eq_South. *Biological and Chemical Oceanography Data System*. BCO DMO, WHOI. iPub: 9 June 1994. Accessed: 17 September 2013. http://www.bco-dmo.org/dataset/2618.

Honjo, S., and J. Dymond (2002), Deep sea sediment trap particle flux, AESOPS/Southern Ocean 1996-1997 Mooring Deployment. *U. S. JGOFS Data System*. iPub: 16 December 2002. Accessed: 09 April 2014. http://usjgofs.whoi.edu/jg/dir/jgofs/southern/.

Honjo, S., J. Dymond, R. Collier and S. J. Manganini (1995), Export production of particles to the interior of the equatorial Pacific Ocean during the 1992 EqPac experiment. *Deep Sea Res. II*, 42(2-3), 831-870.

Honjo, S., and S. Maganini. (1995), Sediment trap data, biogenic particle fluxes North Atlantic Bloom Experiment. *U.S. JGOFS Data System*. iPub: 07 June 1995. Accessed: 09 April 2014. http://usjgofs.whoi.edu/jg/dir/jgofs/nabe/.

Honjo, S., S. J. Manganini, R. A. Krishfield, and R. Francois (2008), Particulate organic carbon fluxes to the ocean interior and factors controlling the biological pump: A synthesis of global

Earth Syst. Sci. Data Discuss., doi:10.5194/essd-2016-22, 2016
Manuscript under review for journal Earth Syst. Sci. Data
Published: 17 June 2016

sediment trap programs since 1983. *Prog. Oceanography*, 76: 217-285. doi:10.1016/j.pocean.2007.11.003.

Kawakami, H., and M. C. Honda (2007), Time-series observation of POC fluxes estimated from ^{234}Th in the northwestern North Pacific. *Deep Sea Res. I*, 54, 1070-1090, doi:10.1016/j.dsr.2007.04.005.

Kuhnt, T., H. Howa, S. Schmidt, L. Marié and R. Scheibel (2013), Flux dynamics of planktonic foraminiferal test in the south-eastern Bay of Biscay (northeast Atlantic margin). *J. Mar. Syst.*, 109-110, S169-S181. doi:10.1016/j.jmarsys.2011.11.026.

Lam, P. J., S.C. Doney, and J.K.B. Bishop (2011), The dynamic ocean biological pump: Insights from a global compilation of particulate organic carbon, CaCO 3, and opal concentration profiles from the mesopelagic. *Global Biogeochem. Cycles*, *25*(3). doi:10.1029/2010GB003868.

Lamborg, C. H., K. O. Buesseler, J. Valdes, C. H. Bertrand, R. Bidigare, S. Manganini, S. Pike, D. Steinberg, T. Trull, and S. Wilson (2008), The flux of bio- and lithogenic material associated with sinking particles in the mesopelagic "twilight zone" of the northwest and North Central Pacific Ocean. *Deep Sea Res. II*, 55, 1540-1563, doi:10.1016/j.dsr2.2008.04.011.

Lee, C. (2011), Sediment Trap Mass Flux, MedFlux. *Biological and Chemical Oceanography Data System*. BCO DMO, WHOI. iPub: 18 October 2011. Accessed: 22 May 2013. http://www.bco-dmo.org/dataset/3561.

Lima, I. D., P.J. Lam, and S.C. Doney (2014), Dynamics of particulate organic carbon flux in a global ocean model. *Biogeosci.*, *11*(4), 1177–1198. doi:10.5194/bg-11-1177-2014.

Lomas, M. W., D. M. Nelson, F. Lipschultz, A. Knap and N. Bates (2009), Trap Flux. *Biological and Chemical Oceanography Data System*. BCO DMO, WHOI. iPub: 03 September 2009. Accessed: 22 May 2013. http://www.bco-dmo.org/dataset/3215.

Lomas, M. W., N. Roberts, F. Lipschultz, J.W. Krause, D. M. Nelson, and N.R. Bates (2009), Biogeochemical responses to late-winter storms in the Sargasso Sea. IV. Rapid succession of major phytoplankton groups. *Deep Sea Res. I*, *56*(6), 892–908. http://doi.org/10.1016/j.dsr.2009.03.004.

Lutz, M. J., K. Calderia, R. B. Dunbar and M. J. Behrenfeld (2007), Seasonal rhythms of net primary production and particulate organic carbon flux to depth describe the efficiency of biological pump in the global ocean. *J. Geophys. Res.*, 112, C100110. doi:10.1029/2006JC003706.

Maritorena, S., D. Siegel, and A. Peterson (2002), Optimization of a semianalytical ocean color model for global-scale applications. *Appl. Opt.*, *41*(15), 2705–2714.

Martin, J. H., G. Knauer, D. Karl, and W. Broenkow (1987), VERTEX: Carbon cycling in the northeast Pacific. *Deep-Sea Res. 1*, *34*, 267–285.

Martin, P., R. S. Lampitt, M. J. Perry, R. Sanders, C. Lee and E. D'Asaro (2011), Export and mesopelagic particle flux during a North Atlantic spring diatom bloom. *Deep Sea Res. I*, 58, 338-349, doi:10.1016/j.dsr.2011.01.006.

Mignot, J., C. de Boyer Montégut, A. Lazar, and S. Cravatte (2007), Control of salinity on the mixed layer depth in the world ocean: 2. Tropical areas. *J. Geophys. Res.*, 112(C10010). doi:10.1029/2006JC003954.

Mohiuddin, M. M., A. Nishimura, Y. Tanaka and A. Shimamoto (2002), Regional and interannual productivity of biogenic components and planktonic foraminiferal fluxes in the

Earth Syst. Sci. Data Discuss., doi:10.5194/essd-2016-22, 2016
Manuscript under review for journal Earth Syst. Sci. Data
Published: 17 June 2016

northwestern Pacific Basin. *Mar. Micropaleontology*, 45, 57-82, doi:10.1016/S0377-8398(01)00045-7.

Mohiuddin, M. M., A. Nishimura, Y. Tanaka and A. Shimamoto (2004), Seasonality of biogenic particle and planktonic foraminifera fluxes: response to hydrographic variability in the Kuroshio Extension, northwestern Pacific Ocean. *Deep Sea Res. I*, 51, 1659-1683, doi:10.1016/j.dsr.2004.06.002.

Montes, E., F. Muller-Karger, R. Thunell, D. Hollander, Y. Astor, R. Varela, I. Soto and L. Lorenzoni (2012), Vertical fluxes of particulate biogenic material through the euphotic and twilight zones in the Cariaco Basin, Venezuela. *Deep Sea Res. I*, 67, 73-84, doi:10.1016/j.dsr.2012.05.005.

Moran, S. B., M. W. Lomas, R. P. Kelly, R. Gradinger, K. Iken and J. T. Mathis (2012), Seasonal succession of net primary productivity, particulate organic carbon export, and autrophic community composition in the eastern Bering Sea. *Deep Sea Res. II*, 65-70, 84-97, doi:10.1016/j.dsr2.2012.02.011.

Morel, A., and J.-F. Berthon, (1989), "Surface pigments, algal biomass, and potential production of the euphotic layer: relationships reinvestigation in view of remote-sensing applications." *Limnol. Oceanogr.*, (8), 1545–1562.

Mouw, C.B., A. Barnett, G. McKinley, L. Gloege, D. Pilcher (2015), Global Ocean Particulate Organic Carbon flux merged with satellite parameters. PANGAEA. doi.pangaea.de/10.1594/PANGAEA.855600.

Mouw, C., and J. Yoder (2010), Optical determination of phytoplankton size composition from global SeaWiFS imagery. *J. Geophys. Res.*, *115*(C12018). doi:10.1029/2010JC006337.

Newton, J. and J. W. Murray (1995a), Poc_pn_trap. *Biological and Chemical Oceanography Data System*. BCO DMO, WHOI. iPub: 27 November 1995. Accessed: 18 September 2013. http://www.bco-dmo.org/dataset-deployment/450839.

Newton, J. and J. W. Murray (1995b), Poc_pn_trap. *Biological and Chemical Oceanography Data System*. BCO DMO, WHOI. iPub: 27 November 1995. Accessed: 18 September 2013. http://www.bco-dmo.org/dataset-deployment/450925.

O'Reilly, J.E., S. Maritorena, M.C. O'Brien, D.A. Siegel, D. Toole, D. Menzies, R.C. Smith, J.L. Muller, B.G. Mitchell, M. Kahru, F.P. Chavez, P. Strutton, G.F. Cota, S.B. Hooker, C.R. McClain, K.L. Carder, F. Muller-Karger, L. Harding, A. Magnuson, D. Phinny, G.F. Moore, J. Aiken, K.R. Arrigo, R. Letelier, and M. Culver (2000), SeaWiFS Postlaunch Calibration and Validation Analyses, Part 3. NASA Tech. Memo. 2000-206892, Vol. 11, S.B. Hooker and E.R. Firestone, Eds., NASA Goddard Space Flight Center, 49 pp.

Rigual-Hernández, A., M. A. Bárcena, R. W. Jordan, R. J. Sierro, J. A. Flores, K. J. S. Meier, L. Beaufort and S. Heussner (2013), Diatom fluxes in the NW Mediterranean: evidence from a 12-year sediment trap record and surficial sediments. *J. Plankton Res*., 35(5), 1109-1225, doi:10.1093/plankt/fbt055.

Smith, W. O. Jr., A. R. Shields, J. C. Dreyer, J. A. Peloquin and V. Asper (2011), Interannual variability in vertical export in the Ross Sea: Magnitude, composition and environmental correlates. *Deep Sea Res. I*, 58, 147-159, doi:10.1016/j.dsr.2010.11.007.

Tesi, T., L. M. Ravaioli, F. Giglio and L. Capotondi (2012), Particulate export and lateral advection in the Antarctic Polar Front (Southern Pacific Ocean): One-year mooring deployment. *J. Mar. Syst.*, 105-108, 70-81, doi:10.1016/j.jmarsys.2012.06.002.

Thurnell, R. C. (2013), Sediment Trap Data. *CARIACO Ocean Time Series Data*. Accessed: 13 September 2013. http://imars.marine.usf.edu/CAR/index.html.

Earth Syst. Sci. Data Discuss., doi:10.5194/essd-2016-22, 2016
Manuscript under review for journal Earth Syst. Sci. Data
Published: 17 June 2016

Open Access Earth System Science Data Discussions

Timothy, D. A., C. S. Wong, J. E. Barwell-Clarke, J. S. Page, L. A. White, and R. W. Macdonald (2013), Climatology of sediment flux and composition in the subarctic Northeast Pacific Ocean with biogeochemical implications. *Prog. Oceanogr.*, 116, 95-129. http://dx.doi.org/10.1016/j.pocean.2013.06.017.

Torres-Valdés, S., A. P. Martin, S. Painter, and R. J. Sanders (2013), Compilation of downward flux observations from sediment trap deployments in the Atlantic Ocean – Contribution to EURO-BASIN’s Data integration. doi:10.1594/PANGAEA.807946, Supplement to: Torres-Valdés, S., S. Painter, A. P. Martin, R. J. Sanders and J. Felden (2014). Data compilation of fluxes of sedimenting material from sediment traps in the Atlantic Ocean. *Earth Syst. Sci. Data*, 6, 123-145. doi:10.5194/essd-6-123-2014.

Earth Syst. Sci. Data Discuss., doi:10.5194/essd-2016-22, 2016
Manuscript under review for journal Earth Syst. Sci. Data
Published: 17 June 2016

Table 1. Summary of dataset parameters

Parameter	Units	Description
Satellite parameters:		
chl_gsm	mg m^{-3}	Chlorophyll *a* concentration
kd490	m^{-1}	Diffuse attenuation coefficient for 490 nm
par	µmol quanta m^{-2} s^{-1}	Photosynthetically available radiation
pp_vgpm	mg C m^{-2} d^{-1}	Net primary production
sfm	%	Microplankton fraction
sst	°C	Sea surface temperature
zeu	m	Base of the euphotic zone
In situ fluxes:		
al_flux	µg m^{-2} d^{-1}	Flux of particulate aluminum
ba_flux	µg m^{-2} d^{-1}	Flux of barium
caco3_flux	mg m^{-2} d^{-1}	Flux of particulate calcium carbonate
chl_flux	mg m^{-2} d^{-1}	Flux of chl
detrital_flux	mg m^{-2} d^{-1}	Flux of detrital particles
mass_flux	mg m^{-2} d^{-1}	Total mass flux
mn_flux	µg m^{-2} d^{-1}	Flux of magnesium
pheo_flux	mg m^{-2} d^{-1}	Flux of phaeopigments
pic_flux	mg m^{-2} d^{-1}	Flux of particulate inorganic carbon
poc_flux	mg m^{-2} d^{-1}	Flux of particulate organic carbon
pon_flux	mg m^{-2} d^{-1}	Flux of particulate organic nitrogen
pop_flux	mg m^{-2} d^{-1}	Flux of particulate organic phosphorus
si_flux	mg m^{-2} d^{-1}	Flux of total particulate silica
sio2_flux	mg m^{-2} d^{-1}	Flux of particulate silica, in the form of SiO_2
sio4_flux	mg m^{-2} d^{-1}	Flux of particulate silica, in the form SiO_4
tc_flux	mg m^{-2} d^{-1}	Flux of total particulate carbon
ti_flux	µg m^{-2} d^{-1}	Flux of titanium
Mixed layer depth climatology:		
mld	m	Mixed layer depth

Earth Syst. Sci. Data Discuss., doi:10.5194/essd-2016-22, 2016
Manuscript under review for journal Earth Syst. Sci. Data
Published: 17 June 2016

Open Access Earth System Science Data Discussions

Table 2. Summary of data sources for POC flux from sediment traps and ^{234}Th, the latter indicated in the description when applicable. Date ranges are from first deployment to last retrieval for a given dataset, but do not necessarily indicate a continuous time series. Sources are listed in order of first deployment.

Latitude/Longitude range	**Date range**	**Description/ Project**	**Reference**
78.9°N – 76.5°S All	1976-07-04 to 2005-05-09	Global collection	*Lutz* et al. [2007] and references therein
81.1°N – 71.1°S 138.9°E – 74.2°W	1982-06-07 to 2007-06-04	Atlantic Ocean Data Compilation	*Torres-Valdés* et al. [2013]
50°N 145°W	1987-09-23 to 2006-06-04	Ocean Station Papa	*Timothy* et al. [2013]
60.3°N – 67.8°S All	1987-06-06 to 2009-08-08	Global collection of ^{234}Th	*Henson* et al. [2011] and references therein
22.8°N 158°W	1988-12-01 to 2010-10-05	HOT, station ALOHA	*Church and Karl* [2013]
32.7°N – 30.6°N 63.1°W – 65.3°W	1988-12-16 to 2011-12-10	BATS	*http://bats.bios.edu, accessed on 27 September 2013*
48°N – 34°N 21°W	1989-04-03 to 1990-04-02	JGOFS North Atlantic Bloom Experiment	*Honjo and Manganini* [1995]
31.8°N 64.2°W	1989-06-09 to 2010-11-09	Ocean Flux Program	*Conte [2015]*
12°N – 12°S 140°W	1992-01-18 to 1993-02-04	JGOFS Equatorial Pacific	*Collier and Dymond* [1994a]; *Collier and Dymond* [1994b]; *Honjo and Dymond* [1994]; *Newton and Murray* [1995a]; *Newton and Murray* [1995b]
43.2°N 5.2°W	1993-10-16 to 2006-01-15	Mediterranean Sea	*Rigual-Hernández* et al. [2013]
17.7°N – 10.0°N 57.8°E – 65.0°E	1994-11-11 to 1995-12-24	JGOFS Arabian Sea	*Honjo* [1999]
10.3°N 64.4°W	1995-11-08 to 2012-12-10	CARIACO	*Thurnell* [2013]
61.5°N – 22.0°N 160°E – 170°W	1996-05-15 to 2005-08-15	Review of ^{234}Th measurements	*Buesseler and Boyd* [2009] and references therein
73.6°S – 76.5°S 176.9°E – 178.0°W	1996-06-12 to 1999-07-25	Ross Sea	*Collier* et al. [2000]
53.0°N – 76.5°N Circumpolar	1996-11-28 to 1998-01-27	JGOFS Southern Ocean	*Honjo and Dymond* [2002]
39°N – 25°N 147°E – 137°E	1997-11-19 to 1999-08-12	Kuroshio Extension, Pacific	*Mohiuddin* et al. [2002]

Earth Syst. Sci. Data Discuss., doi:10.5194/essd-2016-22, 2016
Manuscript under review for journal Earth Syst. Sci. Data
Published: 17 June 2016

Latitude/Longitude range	**Date range**	**Description/ Project**	**Reference**
36.7°N – 36.0°N 147°E – 154.9°E	1998-08-29 to 2000-08-29	Kuroshio Extension, Pacific	*Mohiuddin* et al. [2004]
44°N 155.1°E	1998-11-02 to 1999-05-26	North Pacific	*Honda* et al. [2002]
62.6°S 178.1°W	1999-02-12 to 2001-09-17	Antarctic Polar Front	*Tesi* et al. [2012]
77.0°S – 77.8°S 172.5°W – 180°W	2001-12-22 to 2006-02-03	Ross Sea, Antarctica	*Smith* et al. [2011]
51°N – 39°N 155°E – 165°E	2002-10-16 to 2005-03-06	NW Pacific, ^{234}Th	*Kawakami and Honda* [2007]
43.3°N 7.7°E	2003-03-06 to 2005-04-28	MedFlux, Mediterranean Sea	*Lee* [2011]
33.6°N 118.4°W	2004-01-07 to 2008-06-19	Southern California Bight	*Collins* et al. [2011]
34.9°N – 29.6°N 58.2°W – 67.2°W	2004-02-22 to 2005-03-13	New Production During Winter Convective Mixing Events	*Lomas* et al. [2009]
47.0°N – 22.8°N 161°E – 158°W	2004-06-22 to 2005-08-10	VERTIGO, Pacific	*Lamborg* et al. [2008]
47°N – 30°N 145°E – 160°E	2005-03-21 to 2011-07-24	OceanSITES, K2 and S1, NW Pacific	*Honda* [2012]
44.6°N 2.8°W	2006-06-22 to 2006-06-26	Bay of Biscay	*Kuhnt* et al. [2013]
10.3°N 64.4°W	2007-02-28 to 2008-12-31	CARIACO	*Montes* et al. [2012]
62.3°N – 55.3°N 167.9°W – 176.8°W	2008-03-30 to 2008-07-03	Bering Sea	*Moran* et al. [2012]
61.1°N 26.5°W	2008-05-05 to 2008-05-19	North Atlantic Spring Bloom	*Martin* et al. [2011]

Earth Syst. Sci. Data Discuss., doi:10.5194/essd-2016-22, 2016
Manuscript under review for journal Earth Syst. Sci. Data
Published: 17 June 2016

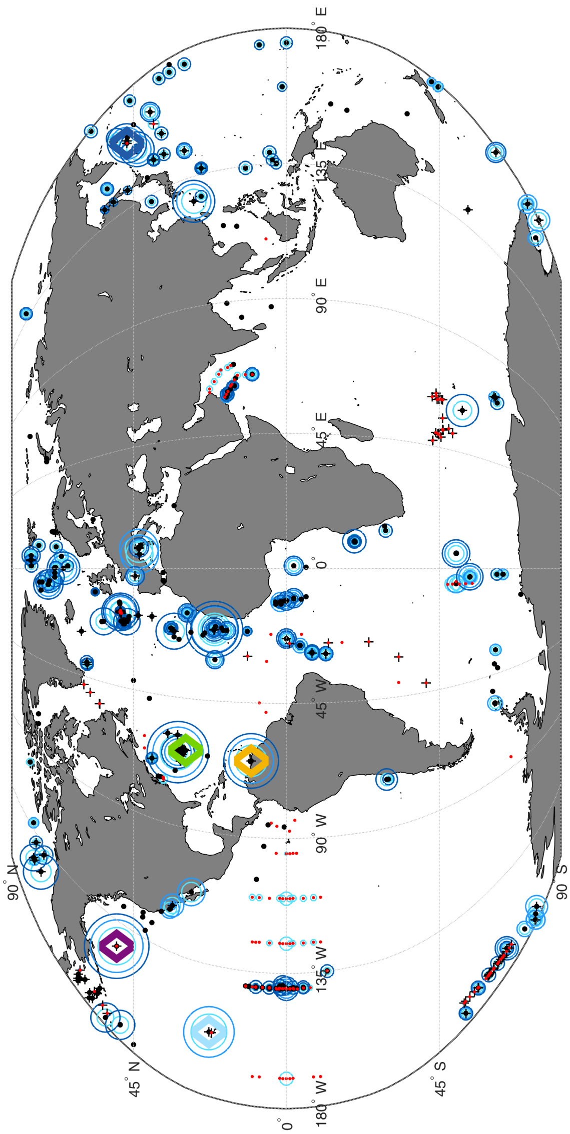

Figure 1. Geographical distribution of POC flux observations at 483 independent sites. The size of the circle indicates the length of the data record at a given site. The color of the circles indicate the depth of observation, where light blue is ≤100 m, medium blue is >100 m and ≤1000 m, and dark blue is >1000 m. The location of sediment trap and ^{234}Th data are indicated in black and red, respectively. Plus symbols (+) indicate which observations are coincident with the ocean color record (i.e. September 1997 – present). The diamonds highlight the locations of time series sites; BATS/OFP (green, 14%), CARIACO (orange, 10%), K2 (dark blue, 2%), OSP (purple, 7%) and HOT (light blue, 3%) account for 36% of the data record.

Earth Syst. Sci. Data Discuss., doi:10.5194/essd-2016-22, 2016
Manuscript under review for journal Earth Syst. Sci. Data
Published: 17 June 2016

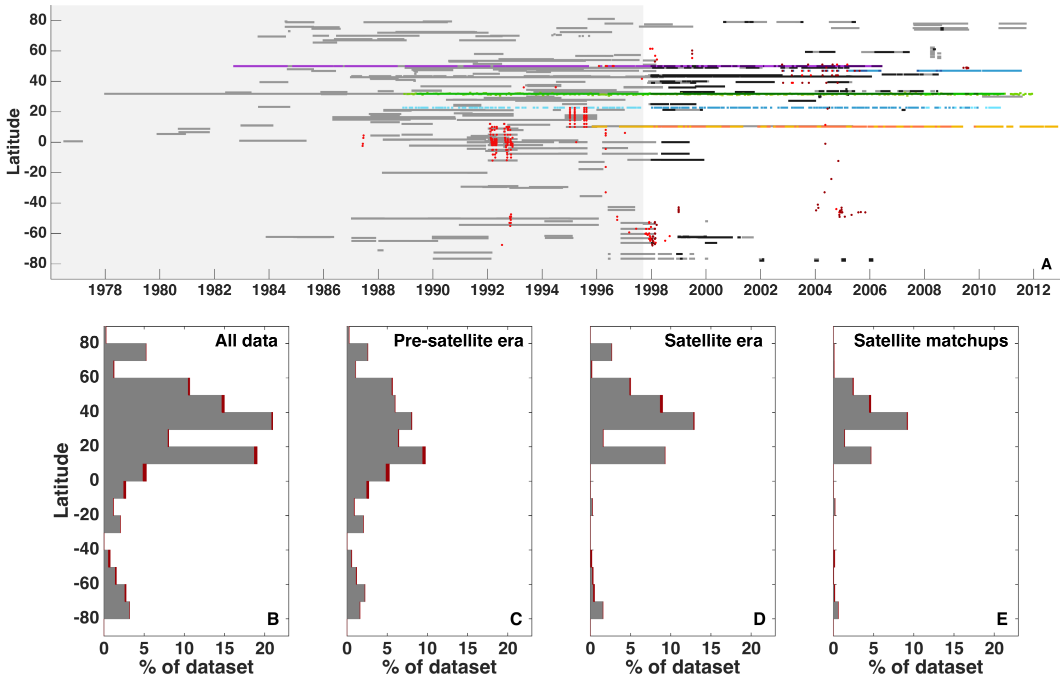

Figure 2. Latitudinal distribution of POC flux observations. (A) The temporal distribution indicates observations prior to (shaded gray) and during the satellite era (right panel). The length of each bar represents a sediment trap deployment; note some bars may overlap. Time series locations are denoted by color as in Figure 1. ^{234}Th data are differentiated in all subplots (red) from observations collected with sediment traps (gray). Observations coincident with satellite NPP and S_{fm} are indicated with darker bars. (B) The percentage of total observations binned by every ten degrees of latitude. (C) Observations prior to the continuous satellite era (before September 1997). (B) Observations collected during the continuous satellite era (beginning September 1997). (C) Observations with coincident satellite imagery within the same month of observation.

Earth Syst. Sci. Data Discuss., doi:10.5194/essd-2016-22, 2016
Manuscript under review for journal Earth Syst. Sci. Data
Published: 17 June 2016

Open Access Earth System Science Data Discussions

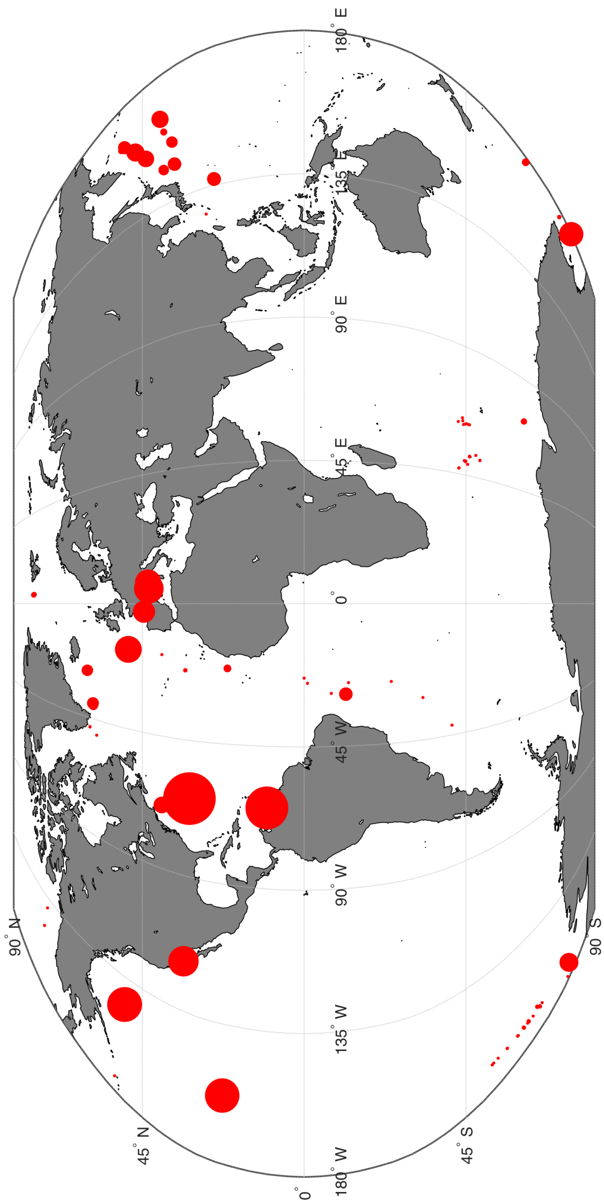

Figure 3. Spatial distribution of coincident satellite and POC flux observations. The size of the circle represents that number of coincident observations.

Earth Syst. Sci. Data Discuss., doi:10.5194/essd-2016-22, 2016
Manuscript under review for journal Earth Syst. Sci. Data
Published: 17 June 2016

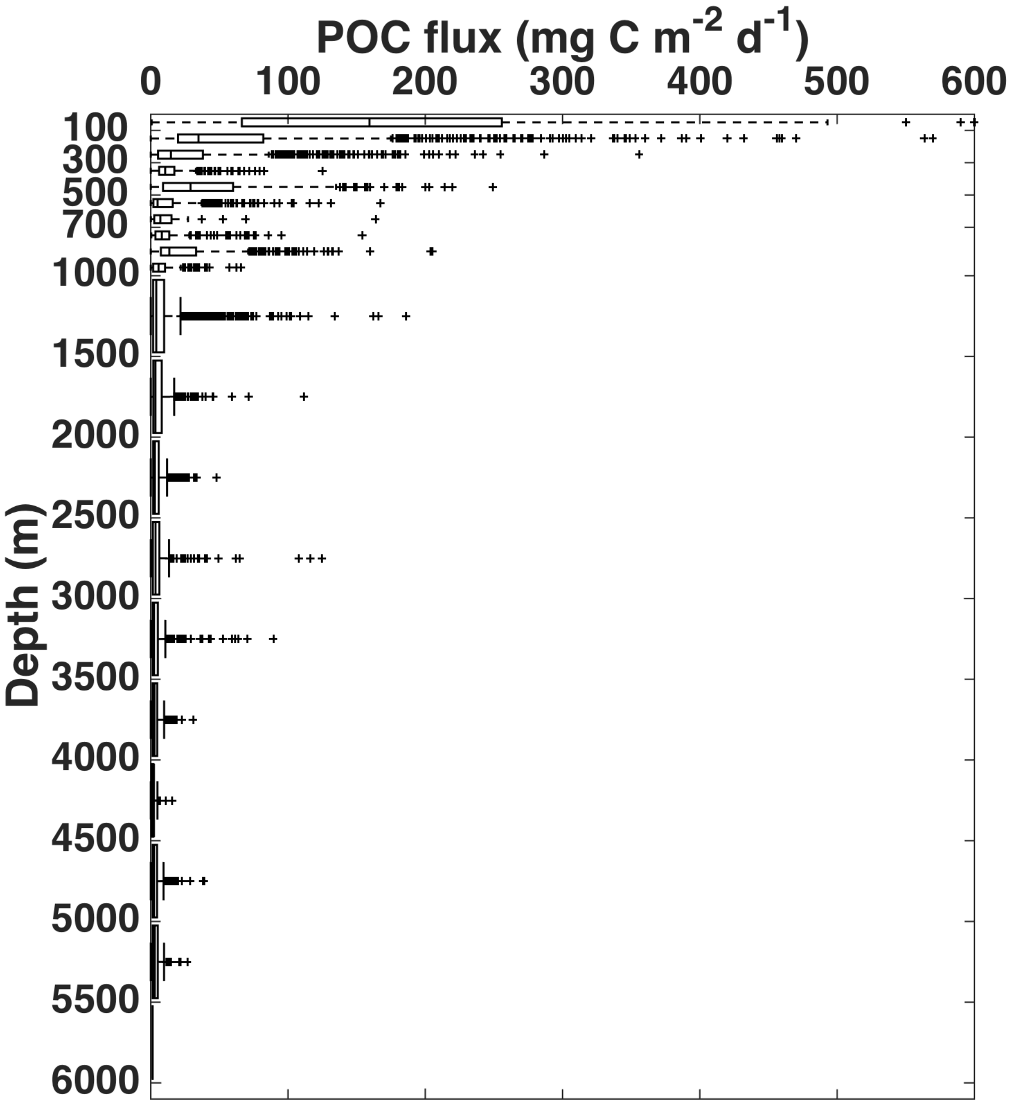

Figure 4. Global POC flux variability with depth. POC flux observations are binned every 100 m in the upper 1000 m and every 500 m throughout the rest of the water column. There are 8 data points not represented on the plot, as they were significantly higher than the majority of the dataset. These values were observed <225 m and are 620, 660, 677, 694, 830, 852, 950 and 1238 mg C m^{-2} d^{-1}.

Earth Syst. Sci. Data Discuss., doi:10.5194/essd-2016-22, 2016
Manuscript under review for journal Earth Syst. Sci. Data
Published: 17 June 2016

Open Access Earth System Science Data Discussions

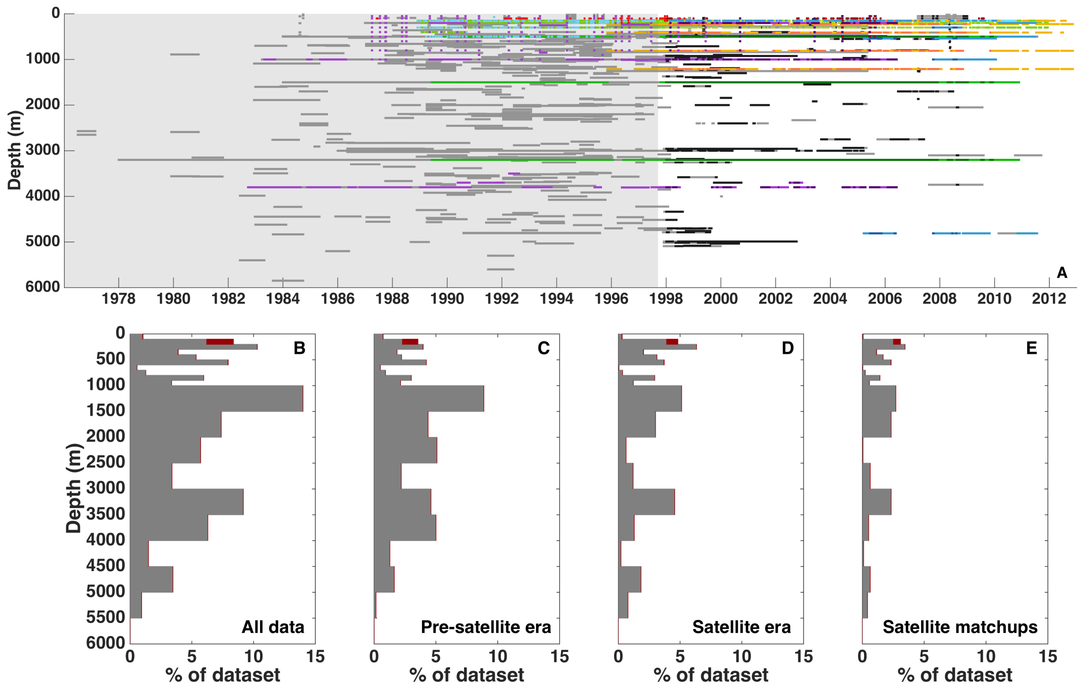

Figure 5. Depth distribution of POC flux observations. The percentage of total observations was binned every 100 m in the upper 1000 m and every 500 m throughout the rest of the water column. (A) The temporal distribution indicates observations prior to (shaded gray) and during the satellite era (right panel). (B) The percentage of depth dinned total observations. (C) Observations prior to the continuous satellite era (before September 1997). (B) Observations collected during the continuous satellite era (beginning September 1997). (C) Observations with coincident satellite imagery within the same month of observation. Temporal depth distribution is indicated with identical coloration as in Figure 2.